

A Review and Evaluation of the Phase Equilibria, Liquid-Phase Heats of Mixing and Excess Volumes, and Gas-Phase *PVT* Measurements for Nitrogen + Methane

A. J. Kidnay,^{a)} R. C. Miller,^{b)} E. D. Sloan,^{a)} and M. J. Hiza

Chemical Engineering Science Division, Center for Chemical Engineering, National Bureau of Standards, Boulder, Colorado 80303

The available experimental data for vapor-liquid equilibria, heat of mixing, change in volume on mixing for liquid mixtures, and gas-phase *PVT* measurements for nitrogen + methane have been reviewed and where possible evaluated for consistency. The derived properties chosen for analysis and correlation were liquid mixture excess Gibbs free energies, and Henry's constants.

Key words: binary mixtures; excess volumes; heat of mixing; nitrogen + methane; vapor-liquid equilibria.

Contents

1. Introduction	682	10. Saturated liquid mixture excess volumes V^E versus temperature T for nearly equimolar $N_2 + CH_4$ mixtures	690
2. Notation	682	11. Deviations between modified hard-sphere model excess volumes V_{CALC}^E and experimental excess volumes V_{EXPR}^E versus temperature T for nearly equimolar $N_2 + CH_4$ liquid mixtures at pressures below 2 MPa.	690
3. Pure Fluid Properties	682	12. Deviations between modified hard-sphere model excess volumes V_{CALC}^E and experimental excess volumes V_{EXPR}^E versus pressure P for nearly equimolar $N_2 + CH_4$ liquid mixtures at temperatures from 96 to 120 K	691
4. Evaluation of Experimental Data	685	13. Percentage deviations between experimental molar densities and molar densities calculated by an extended corresponding states model versus density at temperatures between 270 and 323 K ..	691
4.1. Low-Temperature Phase Equilibria and Heats of Mixing	685	14. Percentage deviation between experimental molar densities and molar densities calculated by an extended corresponding states model versus density at 473 K	692
4.2. High-Temperature Phase Equilibria (Including Critical Locus)	686	15. K -value correlation for the $N_2 + CH_4$ system ...	692
4.3. Liquid Excess Volumes	689	16. Pressure-composition correlation for the $N_2 + CH_4$ system	693
4.4. Gas-Phase <i>PVT</i> Data	691		
5. Summary	692		
6. Acknowledgment	693		
7. References	693		
Appendix A. Calculational Method Used to Obtain g^E Values from <i>PTxy</i> Data	694		
Appendix B. Isotherm Generation from the Data of Bloomer and Parent (Ref. 7)	694		
List of Figures			
1. Comparison of g^E from P, T, x (closed symbols) and P, T, x, y (open symbols)	686		
2. Excess Gibbs energy values from P, T, x measurements	686		
3. Henry's constants	687		
4. The enhancement factor as a function of the pressure difference, $P - P_{CH_4}^s$	688		
5. The enhancement factor as a function of the pressure difference, $P - P_{CH_4}^s$	688		
6. The pressure difference as a function of liquid-phase concentration at 130 K	688		
7. The pressure difference as a function of liquid-phase concentration at 172 K	689		
8. The critical locus of the $N_2 + CH_4$ system	689		
9. The critical locus of the $N_2 + CH_4$ system	689		
List of Tables			
1. Survey of experimental data for vapor-liquid equilibria, heats of mixing, and volume changes on mixing for nitrogen + methane	683		
2. Fixed-point conditions for nitrogen and methane from Refs. 43 and 44	684		
3. Comparison of experimental (exp) vapor pressures with those listed in Refs. 43 and 44	684		
4. Equimolar excess Gibbs energy for $N_2 + CH_4$..	685		
5. Mutually consistent isothermal VLE and h^E data at temperatures below 126 K	686		
6. Henry's constants	687		
7. Mutually consistent isothermal VLE data at temperatures above 126 K	689		
B-1. Summary of Fit of Bloomer and Parent's N_2-CH_4 VLE Data	694		

^{a)}Department of Chemical Engineering and Petroleum Refining, Colorado School of Mines.

^{b)}Department of Chemical Engineering, Washington State University.

© 1985 by the U.S. Secretary of Commerce on behalf of the United States. This copyright is assigned to the American Institute of Physics and the American Chemical Society.

Reprints available from ACS; see Reprints List at back of issue.

1. Introduction

This paper is a continuation of previous work^{1,2} on the review, evaluation, and correlation of phase equilibria and related data on industrially important binary systems of fluids. The first system considered was methane + ethane,¹ the second was methane + propane,² and the present work is concerned with the nitrogen + methane system. These are three of the most important systems related to the natural gas industry.

The methods used to evaluate and correlate data were described in detail in the previous papers,^{1,2} and thus, where possible, discussion of these techniques has been kept to a minimum in the present manuscript. The units for physical quantities have been consistently given in SI, although the literature data appear in many diverse systems. The conversions used in this work are as follows:

$$P/\text{MPa} = 0.1 P/\text{bar} = 0.101\,325 P/\text{atm} \\ = 0.006\,894\,8 P/\text{psia}, \quad (1)$$

$$T/\text{K} = T/^{\circ}\text{C} + 273.15 = T/^{\circ}\text{R}/1.8 \\ = (T/^{\circ}\text{F} + 459.67)/1.8. \quad (2)$$

The experimental measurements for vapor-liquid equilibria (VLE), heat of mixing in the liquid phase, volume change in mixing in the liquid phase, and gas-phase PVT measurements were located using the recent bibliography of Hiza, Kidnay, and Miller,³ and the references are summarized in Table 1.

2. Notation

Symbols

A, B, C	= numerical constants
f	= fugacity
g^E	= excess Gibbs energy
H	= Henry's constant
h^E	= excess enthalpy or heat of mixing
j_{12}, k_{12}	= equation-of-state interaction constants, dimensionless
K	= y/x
P	= pressure

R	= gas constant
T	= absolute temperature
V	= molar volume
V^E	= excess volume
\bar{V}	= partial molar volume
\bar{V}^{∞}	= partial molar volume at infinite dilution
x	= liquid mole fraction
y	= vapor mole fraction
Z	= PV/RT
γ	= activity coefficient, dimensionless
ϕ	= fugacity coefficient, dimensionless

Subscripts

1	= nitrogen
2	= methane
c	= critical
i	= component i

Superscripts

$^{\circ}$	= standard state
P°	= evaluated at the reference pressure $P^{\circ} = 0$
L	= liquid
S	= saturation conditions
V	= vapor

3. Pure Fluid Properties

Accurate pure fluid data are absolutely essential in both consistency testing and correlational work. Fortunately, the thermophysical properties of nitrogen and methane have been correlated recently by Jacobsen *et al.*⁴³ and Goodwin,⁴⁴ respectively. The properties at the triple point, normal boiling point, and critical point are summarized in Table 2.

A comparison of the vapor pressures measured in the vapor-liquid studies of Table 1 with the data of Refs. 43 and 44 is shown in Table 3. The number of significant digits in Table 3 is larger than justified by some of the experimental measurements, but the numbers are retained to avoid round-off error. There are no large discrepancies from which definite conclusions can be drawn concerning sample impurity, or temperature and pressure measurement problems.

Table 1. Survey of experimental data for vapor-liquid equilibria, heats of mixing, and volume changes on mixing for nitrogen + methane

<u>Vapor-Liquid Equilibria</u>			
Reference	Approximate Temperature Range, K	Approximate Pressure Range, 10^5 Pa	Comments
McTaggart and Edwards (1919) [4]	77 to 109	1	
Torocheshnikov and Levius (1939) [5]	89 to 133	0 to 24	
Vellinger and Pons (1943) [6]	90	0 to 1	graphs only
Bloomer and Parent (1952), (1953) [7]	91 to 191	1 to 48	
Cines, Roach, Hogan and Roland (1953) [8]	100 to 172	1 to 44	
Bloomer, Eakin, Ellington and Gami (1955) [9]	100 to 187	7 to 48	graphs only
Fastovskii and Petrovskii (1957) [10]	90 to 150	1 to 16	
Brandt and Stroud (1958) [11]	129 to 179	34	
Ellington, Eakin, Parent et al. (1959) [12]	79 to 187	1 to 48	
Jones and Rowlinson (1963) [13]	140 and 155	----	Tc-x only
Cheung and Wang (1964) [14]	92 to 124	0 to 4	
Spro and Prausnitz (1966) [15]	91	0 to 4	
Chang and Lu (1967) [16]	122, 171	3 to 49	
Fuks and Bellemans (1967) [17]	84 to 89	1 to 3	P-x only
Lu et al. (1969) [18]	135	5 to 40	
Forg and Wirtz (1970) [19]	80 to 180	1 to 100	graphs only
Skripka et al. (1970) [20]	113	----	
Miller, Kidnay and Hiza (1973) [21]	112	2 to 13	
Parrish and Hiza (1974) [22]	95 to 120	0 to 25	
Stryjek, Chappellear, Kobayashi (1974) [23]	113 to 183	1 to 50	
Kidnay, Miller, Parrish, Hiza (1975) [24]	112 to 180	2 to 49	
Wilson (1975) [25]	111	1 to 15	P-x only
McClure et al. (1976) [26]	91	0 to 4	P-x only
<u>Heats of Mixing in the Liquid Phase</u>			
McClure, et al. (1976) [26]	92 to 105		
<u>Changes in Volume on Mixing in the Liquid Phase</u>			
Reference	Approximate Temperature Range, K	Composition Range, mole %	Comments
Blagoi (1959) [27]	90	6 to 89% N_2	
Fuks and Bellemans (1967) [28]	79 to 93	20 to 72% N_2	V^E at 91 K
Liu and Miller (1972) [29]	91 to 115	51% N_2	
Rodosevich and Miller (1973) [30]	91 to 115	5 to 15% N_2	
Hiza, Haynes and Parrish (1977) [31]	95 to 140	5 to 49% N_2	
Nunes da Ponte, Streett and Staveley (1978) [32]	110 to 120	32 to 71% N_2	compressed liquid to 138 MPa
Singh and Miller (1978) [33]	100 to 115	11 to 91% N_2	V^E from dielectric constants to 20 MPa
Singh and Miller (1979) [34]	100 to 115	11 to 91% N_2	V^E from dielectric constants to 50 MPa
<u>Gas Phase PVT Data</u>			
Reference	Approximate Temperature Range, K	Pressure Range, 10^5 Pa	Composition Range, mole %
Roe (1972) [4]	155 to 291	up to 95	28, 52 % N_2
Bloomer and Parent (1953) [7]	110 to 191	up to 50	0 to 70 % N_2
Keyes and Burks (1928) [35]	273 to 473	29 to 330	30, 70 wt % N_2
Mason and Eaker (1961) [36]	289	1	50 % N_2
Blake, Bretton and Dodge (1965) [37]	300	300 to 500	2 to 50 % N_2
Brewer (1967) [38]	273	2	50 % N_2
Semenova, Emelyanova, Tsimmerman, and Tsiklis (1979) [40]	323 to 473		25 to 75 % N_2
Straty and Diller (1980) [41]	130 to 320		30 to 70 % N_2
Haynes and McCarty (1983) [42]	150 to 320		30 to 70 % N_2

Table 2. Fixed point conditions for nitrogen and methane from references 43 and 44

	N ₂	CH ₄
Triple Point		
T/K	63.15	90.68
P/10 ⁵ Pa	0.1253	0.1174
Normal Boiling Point		
T/K	77.35	111.63
P/10 ⁵ Pa	1.01325	1.01325
Critical Point		
T/K	126.20	190.56
P/bar	33.99	45.99
ρ/mol L ⁻¹	11.21	10.0

Table 3. Comparison of experimental (exp) vapor pressures with those listed in references 43 and 44

P(exp)	N ₂ vapor pressure (pressures are in 10 ⁵ Pa)			Temperature/K
	P(ref)	P(exp)-P(ref)	% error in P	
Bloomer and Parent (7)				
16.800	16.922	-0.122	-0.72	112.51
31.400	31.108	0.292	0.93	124.37
8.140	8.171	-0.031	-0.38	100.69
26.140	26.113	0.027	0.10	120.77
7.370	7.398	-0.028	-0.38	99.26
Cines et al. (8)				
7.450	7.631	-0.181	-2.43	99.70
15.400	15.449	-0.049	-0.32	110.90
15.500	15.627	-0.127	-0.82	111.10
27.700	28.022	-0.322	-1.16	122.20
33.000	33.661	-0.661	-2.00	126.00
Spraw and Prausnitz (15)				
3.826	3.818	0.008	0.20	90.67
Fuks and Bellemans (17)				
3.889	3.926	-0.037	-0.96	91.00
Parrish and Hiza (22)				
5.400	5.411	-0.011	-0.21	95.00
7.778	7.787	-0.009	-0.12	100.00
10.835	10.843	-0.008	-0.07	105.00
14.680	14.677	0.003	0.02	110.00
19.389	19.396	-0.007	-0.04	115.00
25.128	25.131	-0.003	-0.01	120.00
Stryjek et al. (23)				
31.800	31.544	0.256	0.80	124.65
27.800	27.804	-0.004	-0.01	122.04
18.100	18.079	0.021	0.12	113.71
Wilson (25)				
15.38	15.48	-0.10	-0.65	110.93
McClure et al. (26)				
3.814	3.822	-0.008	-0.21	90.68
Bloomer and Parent (7)				
0.579	0.568	-0.007	-1.29	105.38
0.985	0.991	-0.006	-0.56	111.36
1.422	1.423	-0.001	-0.07	115.92
2.207	2.211	-0.004	-0.20	122.04
2.624	2.539	0.075	2.86	124.10
5.193	5.166	0.027	0.53	135.91
9.347	9.336	0.011	0.12	147.62
9.758	9.733	0.025	0.25	148.52
12.610	12.601	0.009	0.07	154.33
13.760	13.697	0.063	0.46	156.30
15.500	15.484	0.016	0.10	159.28
18.770	18.733	0.037	0.20	164.12
24.320	24.298	0.022	0.09	171.16
29.940	29.914	0.026	0.09	177.16
31.840	31.845	-0.005	-0.02	179.03
36.080	36.022	0.058	0.16	182.80
39.950	39.851	0.099	0.25	185.97
43.140	43.044	0.096	0.22	188.43
45.800	45.666	0.134	0.29	190.33
46.070	45.981	0.089	0.19	190.55
Spraw and Prausnitz (15)				
0.117	0.117	-0.000	-0.24	90.67
Chang and Lu (16)				
24.690	24.533	0.157	0.64	171.43
Fuks and Bellemans (17)				
1.430	1.431	-0.001	-0.09	116.00
0.122	0.122	-0.000	-0.28	91.00
Parrish and Hiza (22)				
0.199	0.199	-0.000	-0.05	95.00
0.343	0.345	-0.002	-0.62	100.00
0.565	0.566	-0.001	-0.12	105.00
0.884	0.884	0.000	0.00	110.00
1.327	1.326	0.001	0.10	115.00
1.919	1.919	0.000	0.00	120.00
Stryjek et al. (23)				
36.500	36.430	0.070	0.19	183.15
30.400	30.350	0.050	0.16	177.59
25.100	25.069	0.031	0.12	172.04
16.500	16.542	-0.042	-0.25	160.93
10.300	10.329	-0.029	-0.28	149.82
5.960	5.919	0.041	0.68	138.44
3.190	3.176	0.014	0.43	127.59
2.210	2.211	-0.001	-0.06	122.04
1.200	1.198	0.002	0.13	113.71
McClure et al. (26)				
0.117	0.117	-0.000	-0.03	90.68
Wilson (25)				
0.965	0.938	0.007	0.73	110.93

4. Evaluation of Experimental Data

Consistency testing of experimental data may be divided into three general categories: internal consistency tests which measure the scatter of imprecision of a single set of measurements, mutual consistency tests which seek to intercompare data from different sources, and thermodynamic consistency tests which attempt to assess the correspondence of a given set of experimental measurements to known thermodynamic relations. It is desirable to use tests from all three categories for evaluation of fluid property data, but often it is difficult or impossible to do so. The variety of experimental methods and the range of operating conditions encountered in experimental measurements generally make it impossible to apply only a single test from each category to all the data for one system. A description of the major categories of experimental vapor-liquid equilibrium data, along with a brief discussion of the types of consistency tests presently available for these data, were presented in the first paper of this series.¹

The evaluation of all the phase equilibrium data for any binary system is not an easily defined task leading to clear-cut conclusions, but it is a process requiring some subjective judgments by the evaluator as to the applicability and interpretation of the various consistency tests. The basic approach to evaluation taken in this paper is not to assess each data set independently by using thermodynamic consistency tests, but rather to intercompare all of the experimental measurements and discard those data that are obviously inconsistent with the majority of the measurements. The use of thermodynamic consistency tests, while highly desirable, is either impossible or impractical for the majority of the experimental measurements of this report.

For evaluation purposes, the data have been divided into four broad categories; low-temperature phase equilibria and heats of mixing, high-temperature phase equilibria, liquid excess volumes, and gas-phase *PVT* measurements. The temperature dividing line selected for the phase equilibria data was the nitrogen critical temperature, 126 K.

4.1. Low-Temperature Phase Equilibria and Heats of Mixing

One of the best techniques for comparing subcritical VLE data is to calculate from the experimental measurements the excess Gibbs energy g^E , and to graph these values at a fixed composition as a function of temperature. This allows not only an intercomparison of VLE data at different temperatures, since obviously the g^E values must lie on a smooth curve, but also a comparison with calorimetric data, as the slope of the curve is related to the excess enthalpy or heat of mixing.

Two methods have been used to obtain g^E ; the first, due to Barker,⁴⁵ requires only isothermal P,x data, while the second uses isothermal P,x,y measurements. The method of Barker has been discussed extensively in the literature^{46,47} and only the briefest description will be given here. The technique requires two basic assumptions: first, the selection of an expression to represent the composition dependence of g^E in the liquid, and second, the choice of an equation of state to

model the gas phase. In this work a three-term Redlich-Kister expression was selected for g^E , while the Peng-Robinson equation of state was used for the vapor phase. The necessary pure fluid properties were obtained from Jacobsen *et al.*⁴³ and Goodwin,⁴⁴ and the necessary liquid excess volumes were estimated from Singh and Miller.³³

The computational scheme is the same as that discussed in Appendix A of Ref. 1, with the substitution of the Peng-Robinson equation for the virial equation. An advantage of Barker's method is that, since vapor-phase mole fractions are not used in the calculation, a comparison of the experimental and calculated y values constitutes a thermodynamic consistency test. However, the use of an equation of state for the vapor phase, which generally requires the introduction of an empirical binary interaction parameter, imposes some uncertainty on conclusions regarding the consistency of the data.

The second method, utilizing all of the experimental information (P,T,x,y), makes use of the standard thermodynamic relation

$$y_i \phi_i P = x_i \gamma_i f_i^\circ$$

to obtain values for the activity coefficient at the system pressure and temperature. The activity coefficients are then converted to zero pressure and used to calculate values of g^E . The details of the calculations are given in Appendix A.

There are 20 references in the literature containing experimental vapor-liquid equilibria (VLE) measurements below the nitrogen critical point, but only one reference for liquid heats of mixing (see Table 1). Some of the 20 references, however, were deemed unsuitable for evaluation, due to the paucity of experimental measurements or the presentation of results only in graphical form. The work of Refs. 4, 6, 10, 14, 19, and 20 are in this category. The measurements of Fastovskii and Petrovskii¹⁰ were done at constant pressure and are not extensive enough to allow cross plotting and evaluation of g^E and were excluded from the evaluation. The dew-point, bubble-point measurements of Bloomer and co-

Table 4. Equimolar excess Gibbs energy for $N_2 + CH_4$

Reference	T/K	$g^E/J \text{ mol}^{-1}$	
		P,T,x,y data	at $x = 0.5$ P,T,x data
Bloomer and Parent (7)	125	201*	---
Cines et al. (8)	100	257	171
	111	196	185
	122	216	216
	126	224	---
Sprow and Prausnitz (15)	90.67	142	146
Chang and Lu (16)	122	161	224
Fuks and Bellemans (17)	91	---	142†
Miller et al. (21)	112.00	200	185
Parrish and Hiza (22)	95.00	199	171
	100.00	189	176
	105.00	192	179
	110.00	194	183
	115.00	201	197
	120.00	212	209
Stryjek et al. (23)	113.71	207	197
	122.04	223	215
Wilson (25)	111	---	196
McClure et al. (26)	90.68	---	172**

*Obtained from isothermal values generated from dew point and bubble point measurements (see Appendix B).

**Value reported by the authors.

†Obtained from the authors correlation of their data from 84 to 91K.

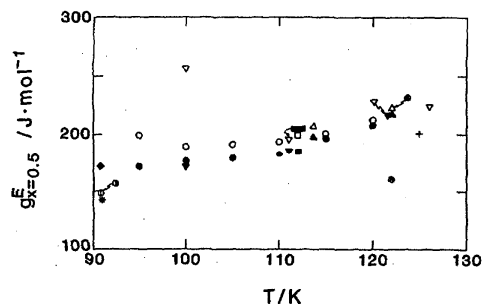


Fig. 1. Comparison of g^E from P,T,x (closed symbols) and P,T,x,y (open symbols).
 ○ Sprow and Prausnitz (15), □ Miller, Kidnay, and Hiza (21),
 ● Parrish and Hiza (22), ▽ Cines et al. (8), ⊙ Chang and Lu (16),
 ▲ Stryjek et al. (23), ◆ McClure et al. (26), * Fuks and Bellemans (17),
 ■ Wilson (25), + Bloomer and Parent (7)

Fig. 1. Comparison of g^E from P,T,x (closed symbols) and P,T,x,y (open symbols).

workers^{7,9,12} were extensive enough to allow limited isothermal data to be generated from the experimental measurements, thus allowing some limited comparisons to be made. The details of the isothermal data generation are in Appendix B. The data of Wilson²⁵ are somewhat unique in that he measured pressure and total composition and then calculated the phase compositions at conditions where gas-phase nonidealities may be substantial (111 K, maximum pressure of 1.5 MPa), but his data are included in the evaluation.

The results of the g^E calculations for the equimolar liquid mixtures using both isothermal P,x data (Barker's method) and P,x,y data are shown in Table 4 and in Figs. 1 and 2. Fuks and Bellemans,¹⁷ Wilson,²⁵ and McClure *et al.*²⁶ did not measure vapor-phase compositions, and thus only Barker's method could be applied to their results. Barker's method was not applied to the Bloomer and Parent⁷ results, since the isothermal data were generated from the original dew-point, bubble-point measurements and thus application of Barker's method was deemed inappropriate. The Cines *et al.*⁸ measurements at the nitrogen critical point, 126 K, did not produce reasonable results when Barker's method was applied and therefore no results are reported at this temperature. Figure 2 also shows the values of g^E obtained from the

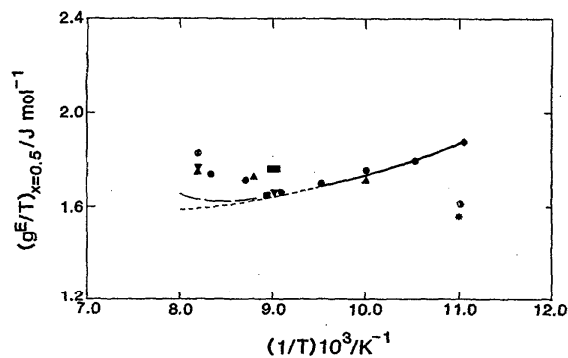


Fig. 2. Excess Gibbs energy values from P,T,x measurements.
 ■ Miller, Kidnay, and Hiza (21), ● Parrish and Hiza (22),
 ▽ Cines et al. (8), ▲ Stryjek et al. (23), ⊙ Chang and Lu (16),
 ○ Sprow and Prausnitz (15), * Fuks and Bellemans (17),
 ◆ McClure et al. (26), ■ Wilson (25), — from h^E
 measurements (see discussion in text)

Fig. 2. Excess Gibbs energy values from P,T,x measurements.

Table 5. Mutually consistent isothermal VLE and h^E data at temperatures below 126 K

Reference		Temperatures/K
Cines et al. (8)	(VLE)	111, 122, 126
Hiller et al. (21)	(VLE)	122.00
Parrish and Hiza (22)	(VLE)	95.00, 100.00, 105.00, 110.00, 120.00
Stryjek et al. (23)	(VLE)	113.71, 122.04
Wilson (25)	(VLE)	111
McClure et al. (26)	(VLE and h^E)	90.68 (VLE), 91.5 and 105.0 (h^E)

heat of mixing measurements of McClure *et al.*²⁶ using the relation

$$\left[\frac{\partial(g^E/T)}{\partial(1/T)} \right]_{P,x} = h^E,$$

and selecting their g^E of 170 J mol⁻¹ at 90.68 K. McClure *et al.* report extensive h^E measurements at 91.5 and 105.0 K, and refer to a single measurement at 122.4 K. If only the measurements at 91.5 and 105.0 K are utilized, a linear relationship between h^E and T must be assumed, and the solid and short-dashed extrapolation shown in Fig. 2 is the result. If the single h^E measurement of 122.4 K (at $x_{N_2} = 0.519$) is combined with the equimolar values at the two lower temperatures, a second-order polynomial relationship can be assumed between h^E and T , resulting in the solid and long-dashed extrapolation of Fig. 2.

The first impression that one might have in viewing Fig. 1 is that considerable disagreement exists between the two methods for obtaining g^E values. This is not really the case however, and in fact for most of the data the agreement between the P,x and P,x,y calculations is excellent, since relatively small changes in the values used for the vapor-phase compositions markedly change the equimolar g^E values. For example, changing the nitrogen vapor composition by 0.005 in the mole fraction results in a change in the equimolar g^E of 20 J mol⁻¹ for the data of Parrish and Hiza at 115 K. It appears, then, that the only isotherms differing significantly (more than ~20 J mol⁻¹) from the bulk of the data shown in Fig. 1 are the 100-K data of Cines *et al.*,⁸ the Sprow and Prausnitz¹⁵ and the Fuks and Bellemans¹⁷ results at approximately 91 K, and the P,x,y calculations of Chang and Lu.¹⁶

In Fig. 2, the only experimental measurements more than 20 J mol⁻¹ away from the h^E and g^E data of McClure *et al.* are those of Sprow and Prausnitz,¹⁵ Chang and Lu,¹⁶ and Fuks and Bellemans.¹⁷

The conclusion, then, is that the data listed in Table 5 are mutually consistent. The data of Bloomer and Parent⁷ are not included in the table, although agreement with the generated 125-K isotherm is satisfactory (see Fig. 2), since, as discussed previously, the original data are dew-point and bubble-point measurements, making definitive comparisons with isothermal measurements unfeasible.

4.2. High-Temperature Phase Equilibria (Including Critical Locus)

The phase equilibria data above 126 K were taken directly from the references, with one exception. The bubble-

Table 6. Henry's constants

Investigator	T/K	Christiansen and Fredenslund			Gunn et al.
		H 10 ⁵ Pa	Δy Avg	No. of collocation points	H 10 ⁵ Pa
Torochoeshnikov and Levius (5)	129.87	78.60	.0480	13	73.67
	132.92	175.23	.1137	10	77.69
Bloomer and Parent (7)	127.59	42.84	-----	---	-----
	130.39	-----	-----	---	45.29
	138.71	55.28	-----	---	-----
	147.05	-----	-----	---	64.31
	150.00	66.27	-----	---	-----
Cines et al. (8)	158.17	-----	-----	---	71.05
	160.93	88.43	-----	---	-----
	133.15	48.97	.0100	11	46.51
	144.26	72.00	.0063	12	63.08
Chang and Lu (16)	155.37	91.48	.0077	9	83.50
	172.04	112.83	.0221	8	120.56
	130.1	-----	-----	---	46.58
Stryjek et al. (23)	171.4	-----	-----	---	79.10
	127.59	35.85	.0067	8	42.00
	138.44	44.91	.0073	11	55.39
	149.82	65.74	.0164	9	66.61
	160.93	65.02	.0170	8	76.50
	172.04	60.75	.0132	8	86.97
Kidnay et al. (24)	177.59	112.11	.0072	8	95.83
	130.00	46.00	.0058	8	46.03
	140.00	57.70	.0047	11	57.14
	150.00	68.77	.0066	8	69.52
	160.00	79.30	.008	8	75.88
	170.00	98.98	.0042	8	84.01
	180.00	102.70	.0088	8	93.96

point (BP)-dew-point (DP) data of Bloomer and Parent⁷ were graphed as well as fit to a second-order expansion of BP or DP pressure in terms of absolute temperature. The latter method, originally suggested by Bloomer and Parent, was determined to yield the most reliable x, y data at a given P and T . The data of Fastovskii and Petrovskii¹⁰ and those of Brandt and Stroud¹¹ taken at isobaric conditions, were excluded from this evaluation since there were insufficient data to permit the generation of isothermal results. Similarly, the data of Lu *et al.*¹⁸ and those of Forg and Wirtz¹⁹ were excluded, since only graphical data were presented.

Four tests were performed on phase equilibria data above 126 K, namely, (1) Henry's constant evaluation by the methods of Gunn, Yamada, and Whitman⁴⁸ and of Christiansen and Fredenslund,⁴⁹ (2) enhancement factor ($y_i P / P_i^s$) versus $(P - P_i^s)$ plots, (3) plots of $(P - P_i^s)$ versus liquid mole

fraction of nitrogen, and (4) orthogonal collocation predictions of y from measured P, x data.⁴⁹

The method of Gunn, Yamada, and Whitman to determine infinite dilution Henry's constants at the methane vapor pressures was discussed in Appendix B of Ref. 1. The computer program, which was obtained directly from Gunn, places a low weighting factor on data at low nitrogen concentrations. Henry's constants from this method are listed in Table 6 and plotted in Fig. 3.

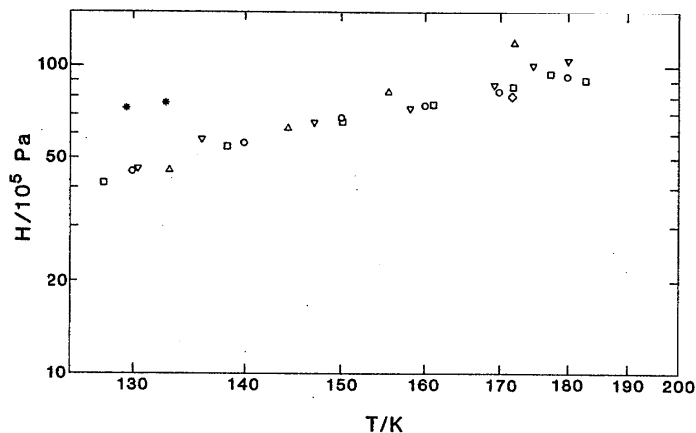
The unsymmetric-convention orthogonal collocation program of Christiansen and Fredenslund⁴⁹ was obtained directly from the authors, as documented in Appendix B of Ref. 1. P, x data along isotherms were processed to calculate consistent y values, which were compared to experimental data. The number of collocation points was chosen to minimize the absolute deviation in y . The results listed in Table 6 indicate that the minimum deviation in y is produced by different numbers of collocation points for different isotherms. Henry's constants were also evaluated from this method, but are somewhat scattered relative to the Gunn method, due to the emphasis placed on the data at the lowest nitrogen concentrations. Henry's constants from both methods are compared in Table 6.

Plots of enhancement factor ($y_i P / P_i^s$) versus $(P - P_i^s)$ provide a rigorous test of low-concentration vapor-phase composition. In a similar manner, plots of $(P - P_i^s)$ versus liquid mole fraction of nitrogen provide a somewhat less sensitive test of low-concentration liquid-phase composition. Both plots should form a straight line that passes through the origin.

The Henry's constant data, obtained using the method of Gunn, Yamada, and Whitman, are represented by the equation

$$\ln H = 5.0684 + 82.5822(1/T) - 31.896.17(1/T)^2,$$

where H is in units of 10⁵ Pa and T is in K. In Fig. 3, the data of Torochoeshnikov and Levius and the 155.4- and 172.05-K isotherms of Cines *et al.* show unacceptable deviations from the others, and were excluded in the above fit.



□ Kidnay et al. (24), ▽ Bloomer and Parent (7), □ Stryjek et al. (23),
△ Cines et al. (8), ◇ Chang and Lu (16), * Torochoeshnikov and Levius (5)

FIG. 3. Henry's constants.

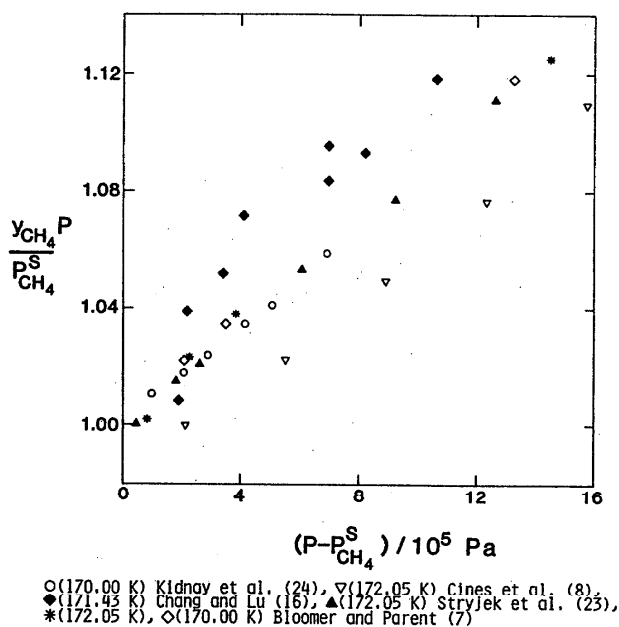


FIG. 4. The enhancement factor as a function of the pressure difference, $P - P_{CH_4}^S$.

The Henry's constants from the orthogonal collocation are not included in either Fig. 3 or the above equation, due to the emphasis on low-concentration data. Table 6 provides the results of the orthogonal collocation program. The data of Chang and Lu could not be processed with the program, probably due to scatter in the experimental data. Data scatter in the table is indicated by large average deviations in calculated versus experimental y values. The 172.04-K isotherm of Cines *et al.* shows unacceptable deviation, as do both isotherms of Torochesnikov and Levius.

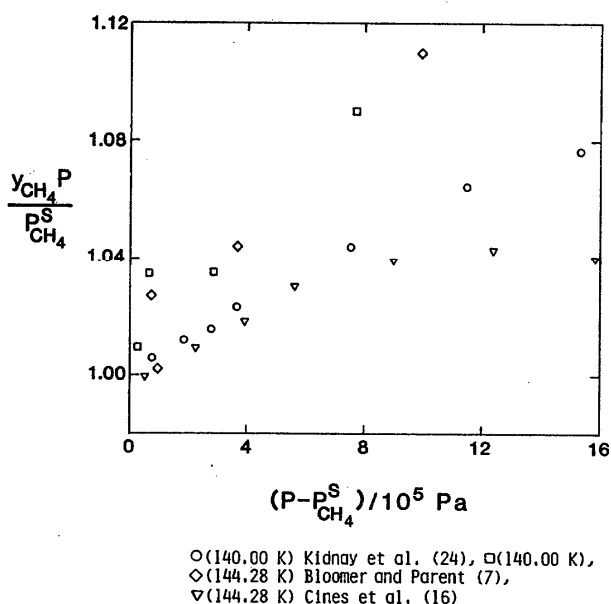


FIG. 5. The enhancement factor as a function of the pressure difference, $P - P_{CH_4}^S$.

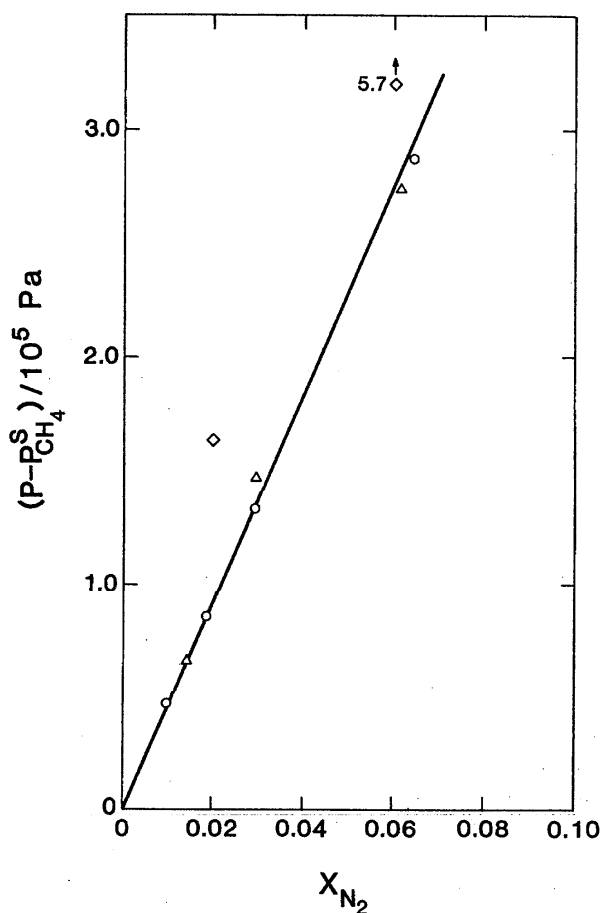
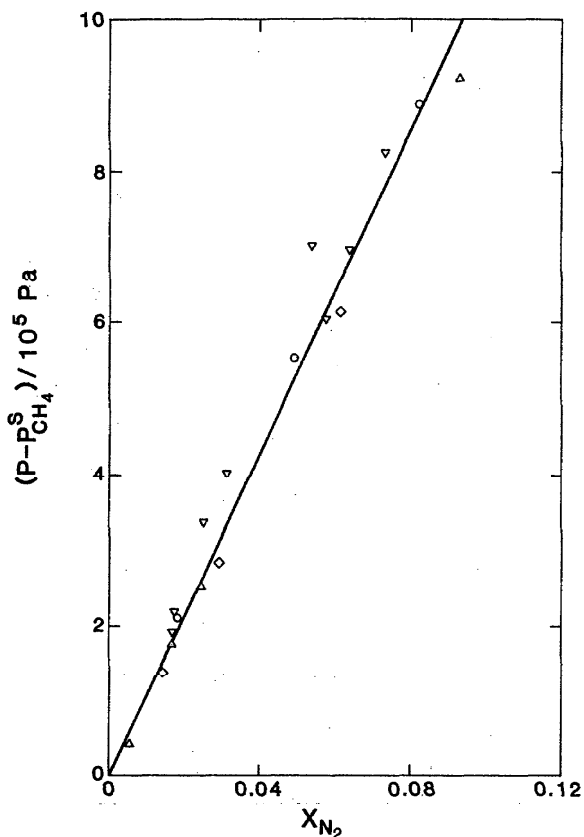


FIG. 6. The pressure difference as a function of liquid-phase concentration at 130 K.

The enhancement factor plot of Fig. 4 combines data at 170, 171.43, and 172.05 K. The plot indicates that the data of Chang and Lu are unacceptably high and the data of Cines *et al.* are unacceptably low. Figure 5 combines data at 140 and 144 K. The data of Bloomer and Parent and the data of Cines *et al.* show unacceptable deviations. Other plots were made at 180, 160, 155.39, 150, 133.17, 130, and 129.87 K, without conclusive results.

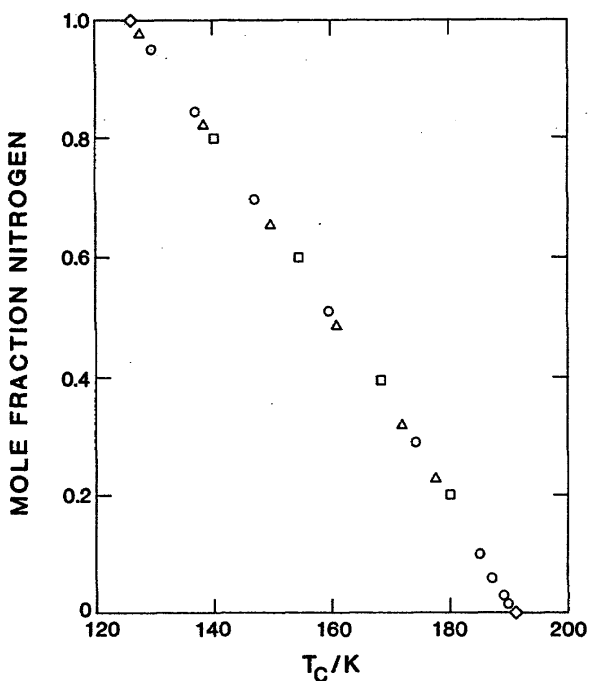
Plots of $(P - P^S)$ versus nitrogen liquid mole fraction were made at 180, 172, 170, 160, 155.4, 150, 144.3, 140, 133, and 130 K. Although these plots were somewhat less sensitive than the enhancement factor plots, a discrimination was obtained for poor data, such as those of Torochesnikov and Levius at 130 K, as shown in Fig. 6. Similarly, Fig. 7 shows the data of Chang and Lu to be unacceptably high at 172 K.

Critical locus data have been reported by Bloomer and Parent,⁷ Jones and Rowlinson,¹³ and Stryjek *et al.*²³ Comparisons of these measurements are shown in Figs. 8 and 9. Jones and Rowlinson measured only temperature and composition, and thus their measurements appear only in Fig. 8. The measurements of Bloomer and Parent compare very favorably with those of Stryjek *et al.* on both figures, but the



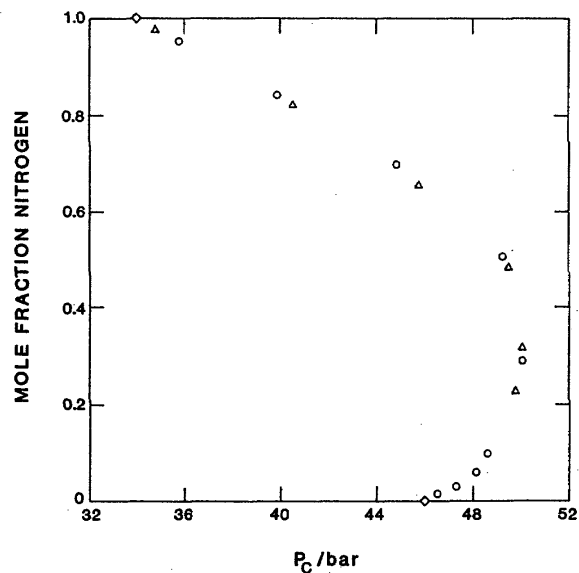
◇ Bloomer and Parent (7), ○ Cines et al. (8),
 △ Stryjek et al. (23), ▽ Chang and Lu (16)

FIG. 7. The pressure difference as a function of liquid-phase concentration at 172 K.



○ Bloomer and Parent (7), □ Jones and Rowlinson (13),
 △ Stryjek et al. (23), ◇ Critical of pure components

FIG. 8. The critical locus of the $N_2 + CH_4$ system.



○ Bloomer and Parent (7), △ Stryjek et al. (23),
 ◇ Critical of pure components

FIG. 9. The critical locus of the $N_2 + CH_4$ system.

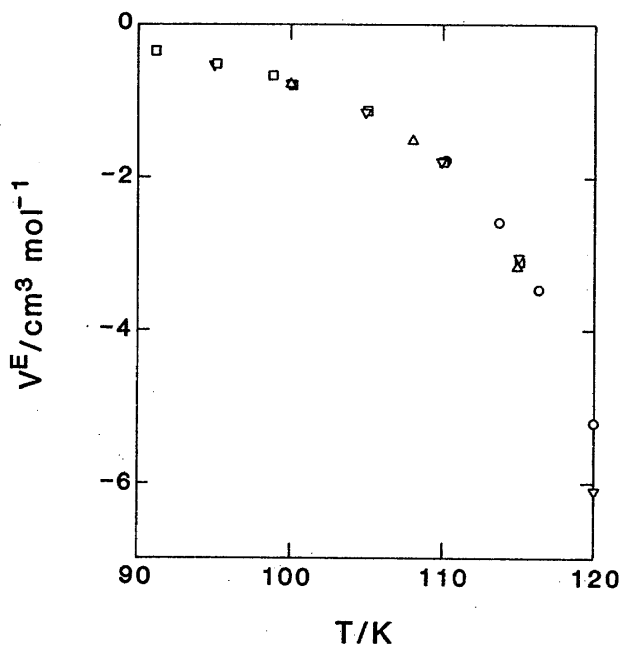
data of Jones and Rowlinson diverge somewhat from the other measurements. For the vapor-liquid equilibria measurements above 126 K, the data listed in Table 7 are mutually consistent and therefore are the most likely to be reliable.

4.3. Liquid Excess Volumes

There are probably more excess volume data for nitrogen + methane than for any other binary system composed of simple molecular species. Liquid mixture excess volumes at pressures near bubble-point conditions have been reported in Refs. 27–34. Saturated liquid excess volumes for equimolar nitrogen + methane from Refs. 29 and 31–34 are intercompared as V^E versus T in Fig. 10. Data from Refs. 27, 28, 30 were not included in this comparison because the equimolar mixture was not studied. Both Ref. 27 and Ref. 28 studies produced V^E versus composition at constant T near 91 K. The Blagoi²⁷ V^E data exhibit an S-shaped curve, positive for nitrogen-rich mixtures and negative for methane-rich mixtures. This behavior is not reproduced by any other study near this temperature. Scatter in the Fuks and Belle-mans²⁸ data make estimation of the equimolar value uncer-

Table 7. Mutually consistent isothermal VLE data at temperatures above 126 K

Reference	Temperatures
Bloomer and Parent (7)	All data except 142 ± 5 K data
Cines et al. (8)	133.17 K
Chang and Lu (16)	130.1 K
Kidnay, et al. (24)	130, 140, 150, 160, 170, 180 K
Stryjek et al. (23)	127.6, 138.5, 149.8, 160.9, 172, 177.6, 183 K



▽Hiza et al. (31), □Liu and Miller (29),
○Nunes da Ponte et al. (32),
△Singh and Miller (34, 35)

FIG. 10. Saturated liquid mixture excess volumes V^E vs temperature T for nearly equimolar $N_2 + CH_4$ mixtures.

tain. Rodosevich and Miller³⁰ present data for methane-rich mixtures only.

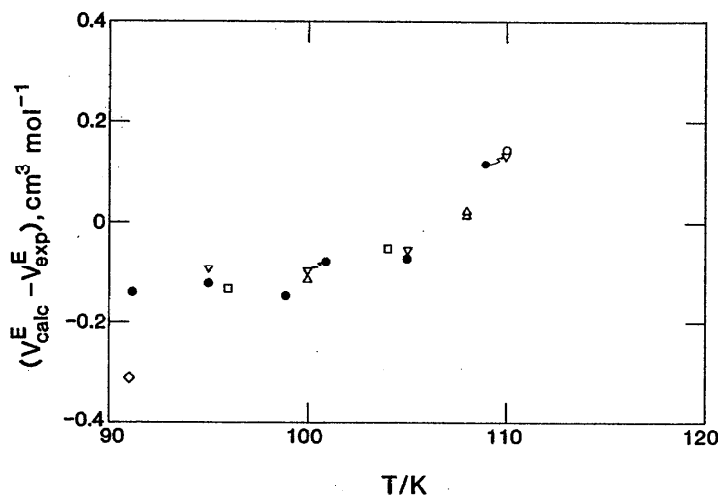
As can be seen from Fig. 10, there is excellent agreement among the four data sets compared, except at 120 K. At this temperature, nitrogen is near its critical temperature, and the excess volume at pressures near saturation is an ex-

tremely strong function of pressure, temperature, and composition. Saturated liquid V^E values at other compositions from Refs. 29–34 are also in good agreement (cf. Hiza et al.³¹).

There have been four liquid volumetric studies in which pressure was also a primary variable.^{32–35,41} References 32–34 reported $V^E(P, T, x)$, while Ref. 41 reported molar volumes as a function of pressure and temperature for three nitrogen + methane mixtures. For the present work, these molar volumes have been used to calculate V^E 's by combining them with component molar volumes from the same apparatus.^{44,50} Values at the exact P and T for each mixture measurement were taken from close fits of each component data set by a 32-term modified BWR equation of state.^{41,51}

The V^E data from Refs. 28, 29–34, and 41 have been simultaneously fit by use of the modified hard-sphere model exactly as described by Singh and Miller.⁵² The Longuet-Higgins and Widom form of their equation was used with component parameters from Tables 1 and 2 of this reference. As suggested by the above authors, data were not used at low pressures at temperatures above 110 K. A total of 245 V^E data points were fit with a standard deviation of $0.061 \text{ cm}^3 \text{ mol}^{-1}$. The two deviation parameters determined from the fit were $k_{12} = 0.0602$ and $j_{12} = 0.0036$.

Figures 11 and 12 show some comparisons of various data sets, all data being plotted as deviations between model calculations and experiment. All data on these plots are at compositions very close to $x = 0.5$, except for the one point from Ref. 28 that is at $x(N_2) = 0.56$. In Fig. 11, deviations are plotted versus temperature, and all data are at pressures less than 2 MPa. Except for the Ref. 28 point, data from all sets are in excellent agreement with each other. There are systematic model deviations from all data, which would become very large if data above 110 K had been included. In Fig. 12, deviations are plotted against pressure, with temperatures



▽Hiza et al. (31), ●Liu and Miller (29), ○Nunes da Ponte et al. (32),
△Singh and Miller (33, 34), □Straty and Diller (41), ◇Fuks and Bellemans (28)

FIG. 11. Deviations between modified hard-sphere model excess volumes V^E_{CALC} and experimental excess volumes V^E_{EXPR} vs temperature T for nearly equimolar $N_2 + CH_4$ liquid mixtures at pressures below 2 MPa.

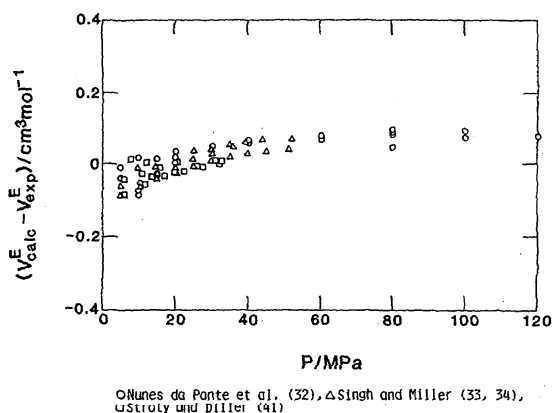


Fig. 12. Deviations between modified hard-sphere model excess volumes V_{CALC}^E and experimental excess volumes V_{EXPR}^E vs pressure P for nearly equimolar $\text{N}_2 + \text{CH}_4$ liquid mixtures at temperatures from 96 to 120 K.

ranging from 96 to 120 K. No data below 5 MPa are shown. Again, the three high-pressure data sets are in good internal agreement (on the order of $\pm 0.04 \text{ cm}^3 \text{ mol}^{-1}$ or $\pm 0.1\%$ of the mixture molar volumes). Small systematic model deviations are again apparent, but they are not divergent at either high or low pressures. It should be noted that the temperature dependence of V^E disappears for this system at pressures greater than about 30 MPa.⁵²

In conclusion, Refs. 29–34 and 41 provide an extensive $V^E(P, T, x)$ data set, which is in good internal agreement. Except for low-pressure data at temperatures above 110 K, these data have been fit by a modified hard-sphere model using two binary parameters (standard deviation = $0.06 \text{ cm}^3 \text{ mol}^{-1}$). As shown on Figs. 11 and 12, there are small systematic deviations between model and experiment. Thus it has not been possible to fit the data completely within the combined experimental uncertainties of the various data sets. Perhaps a more complicated model, such as the 13-constant Redlich–Kister equation used by Singh and Miller^{33,34} could be used for this purpose. Such complicated models are not necessary for intercomparison of the data sets, and they have not been shown to be useful in estimating multicomponent data from binary data fits.

4.4. Gas-Phase PVT Data

Compressed gaseous mixture PVT data are reported in Refs. 7 and 35–42. Brewer³⁸ gives only the nitrogen and methane cross second virial coefficient at 273 K, while Mason and Eakin³⁶ list only the compressibility factor for the equimolar mixture at 1 atm and 288.7 K. The data from Straty and Diller⁴¹ and from Haynes and McCarty⁴² represent a wide-range study in the same laboratory. Results of this study for $x = 0.5$ have been closely fit⁴¹ to a 32-term modified Benedict–Webb–Rubin equation of state.⁵¹ Comparisons have been made⁴¹ between equation-of-state results and the equimolar mixture molar densities of Bloomer and Parent⁷ and of Roe.³⁹ In both cases, agreement was within

$\pm 0.3\%$ in density, which is within the combined experimental uncertainties.

References 37 and 40 also give data for very close to equimolar mixtures at temperatures near 300 K. The data from Blake *et al.*³⁷ are at pressures from 30 to 500 MPa, while the Semenova *et al.*⁴⁰ data are between 200 and 900 MPa. The maximum pressure for any of the data used to develop the equation of state was about 35 MPa. In the present work, calculated densities from the previously developed modified BWR equation were compared with the Ref. 37 data at 323 K and the Ref. 40 data at 299 K. Agreement with the Ref. 37 data is within 0.3% to 30–35 MPa, but diverges to a 12% difference at 500 MPa. Similarly large differences are encountered for the Ref. 40 data, with 6% deviation at 200 MPa and 16% deviation at 900 MPa. It is obvious that the problem involves poor extrapolation of the BWR equation to high pressures.

In an attempt to provide a more meaningful intercomparison of the several data sets, percentage deviations were calculated between experimental molar densities and calculations based on an extended corresponding states model.⁵³

As shown in Refs. 41 and 42, large deviations are encountered at 150 to 250 K with this model. In the present study, only data above 270 K have been intercompared. Slightly different binary interaction parameters were used from those used in Refs. 41 and 42. Data from 270 to 323 K are plotted on Fig. 13 as percentage deviation versus molar density. At densities below about 15 mol cm^{-3} , the temperature and composition dependencies of the deviations are relatively small, and it is easy to see that the data from Refs. 35, 37, 39, 41, and 42 are in good agreement in this region (probably within $\pm 0.3\%$ or better). At higher densities, the temperature, composition, and density effects on the deviations become much larger, and it becomes more difficult to intercompare data. Based on looking at both composition and temperature effects, it appears that the data from Refs. 37 and 40 are actually in good agreement to 25–32 mol cm^{-3} , where the two sets overlap in density.

Data at higher temperatures are reported in Refs. 35 and 40, however, there is no overlap in density (or pressure) for these two sets. Data from these references at 473 K and compositions near $x = 0.5$ are shown in Fig. 14. Deviations from the corresponding states model are large and strongly

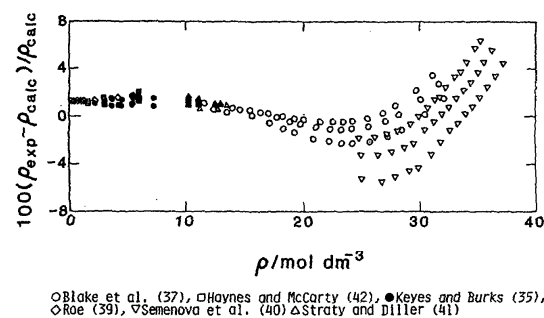
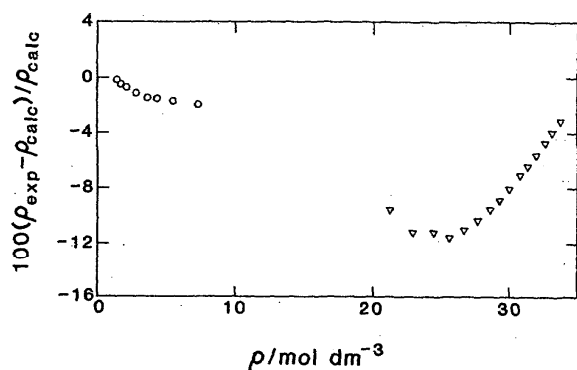


Fig. 13. Percentage deviations between experimental molar densities and molar densities calculated by an extended corresponding states model vs density at temperatures between 270 and 323 K.



○Keyes and Burks (35), ▽Semonova et al. (40)

FIG. 14. Percentage deviation between experimental molar densities and molar densities calculated by an extended corresponding states model vs density at 473 K.

density dependent. It is impossible to draw any conclusions on the consistency of these two data sets at the higher temperatures.

5. Summary

The mutually consistent VLE data, consisting of nine independent investigations covering the temperature region

from the triple point of methane to near the methane critical temperature, are listed in Tables 5 and 7. Graphical correlations of the data in the form of a K -value ($K \equiv y/x$) chart and a pressure-composition chart are presented in Figs. 15 and 16. These figures were originally published in the "LNG Materials and User's Manual," first edition, Natl. Bur. Stand. (U. S.), Boulder, CO 80303 (1977). The computational method used to generate these figures is discussed in Appendix C of Ref. 1. Both SI and engineering units are used with these figures to increase their utility. The critical locus for the figures was taken from Stryjek *et al.*²³

Since only Ref. 26 is available for heats of mixing in the liquid phase, it is not possible to assess the accuracy of the data. However, as shown in Fig. 2, the g^E values from phase equilibria measurements show the same trend as the h^E data, thus indicating at least a good degree of internal consistency.

There are seven sets^{29-34,41} of liquid-phase excess volume measurements that exhibit good internal agreement, but unfortunately no thermodynamic consistency tests are available for intercomparison of the measurements.

The available gas-phase PVT data^{7,35-42} cannot be compared with a rigorous thermodynamic consistency test, but in many cases intercomparison of the densities was possible. At lower densities (below about 15 mol cm^{-3}) Refs. 35, 37, 39, 41, and 42 are in good agreement, and at higher densities the data from Refs. 37 and 40 show good agreement in areas of overlap.

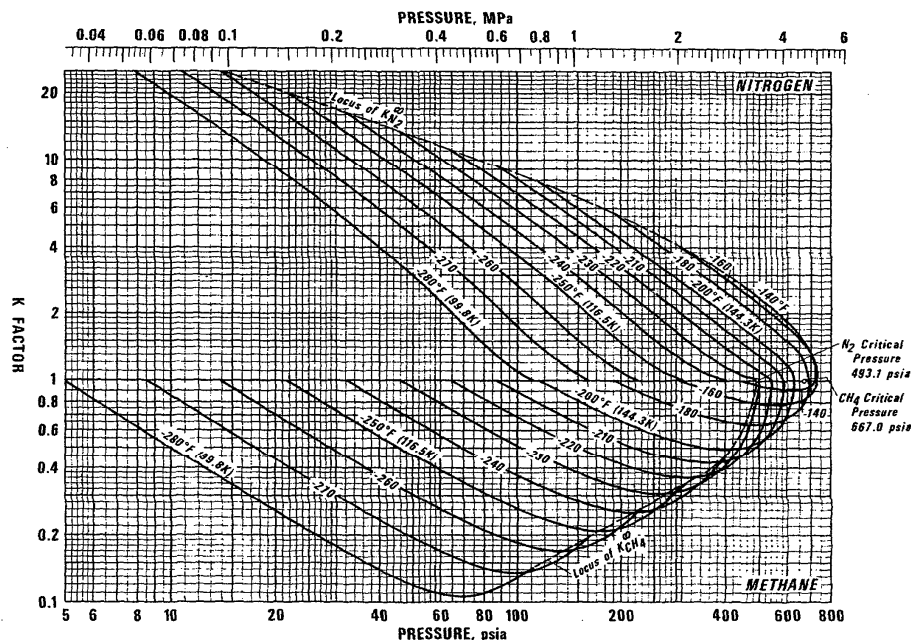
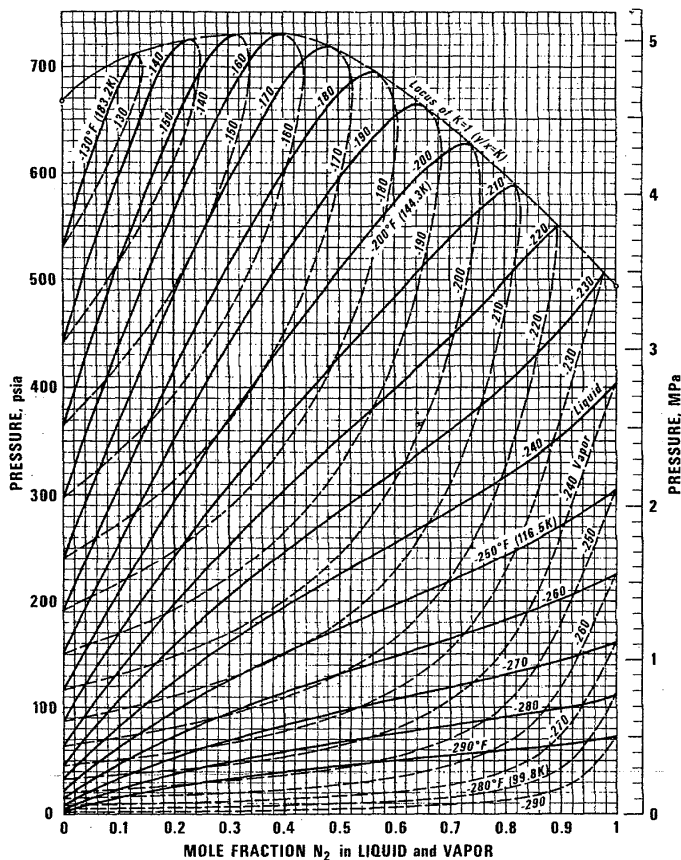


FIG. 15. K -value correlation for the $\text{N}_2 + \text{CH}_4$ system.

FIG. 16. Pressure-composition correlation for the $N_2 + CH_4$ system.

6. Acknowledgment

Financial support for this work was provided by the Office of Standard Reference Data, National Bureau of Standards.

7. References

- ¹M. J. Hiza, R. C. Miller, and A. J. Kidnay, *J. Phys. Chem. Ref. Data* **8**, 799 (1979).
- ²R. C. Miller, A. J. Kidnay, and M. J. Hiza, *J. Phys. Chem. Ref. Data* **9**, 721 (1980).
- ³M. J. Hiza, A. J. Kidnay, and R. C. Miller, *Equilibrium Properties of Fluid Mixtures. 2. A Bibliography of Experimental Data on Selected Fluids* (IFI/Plenum, New York, 1982), p. 246.
- ⁴H. A. McTaggart and E. Edwards, *Trans. R. Soc. Can. Sect. 3* **13**, 47 (1919).
- ⁵N. S. Torocheshnikov and L. A. Levius, *Zh. Khim. Prom.* **16**(1), 19 (1939). This data appears in graphical form in M. Ruheman, *The Separation of Gases* (Oxford University, London, 1949), p. 54.
- ⁶E. Vellinger and E. Pons, *C. R. Acad. Sci.* **217**, 689 (1943).
- ⁷O. T. Bloomer and J. D. Parent, *Inst. Gas Technol. Chicago Res. Bull.* **17** (1952); O. T. Bloomer and J. D. Parent, *Chem. Eng. Prog. Symp. Ser.* **49** (6), 11 (1953); O. T. Bloomer, Ph.D. thesis (Illinois Institute of Technology, 1953).
- ⁸M. R. Cines, J. T. Roach, R. J. Hogan, and C. H. Roland, *Chem. Eng. Prog. Symp. Ser.* **49** (6), 1 (1953).
- ⁹O. T. Bloomer, B. E. Eakin, R. T. Ellington, and D. C. Gami, *Inst. Gas Technol. Chicago Res. Bull.* **21** (1955).
- ¹⁰V. G. Fastovskii and Yu. V. Petrovskii, *Zh. Fiz. Khim.* **31**, 2317 (1957).
- ¹¹L. W. Brandt and L. Stroud, *Ind. Eng. Chem.* **50**, 849 (1958).
- ¹²R. T. Ellington, B. E. Eakin, J. D. Parent, D. L. Gami, and O. T. Bloomer, in *Thermodynamic and Transport Properties of Gases, Liquids and Solids* (McGraw-Hill, New York, 1959), pp. 180-194.
- ¹³I. W. Jones and J. S. Rowlinson, *Trans. Faraday Soc.* **59**, 1702 (1963).
- ¹⁴H. Cheung and D. I.-J. Wang, *Ind. Eng. Chem. Fundam.* **3**, 355 (1964).
- ¹⁵F. B. Sprow and J. M. Prausnitz, *AIChE J.* **12**, 780 (1966).
- ¹⁶S.-D. Chang and B. C.-Y. Lu, *Chem. Eng. Prog. Symp. Ser.* **63** (81), 18 (1967).
- ¹⁷S. Fuks and A. Bellemans, *Bull. Soc. Chim. Belg.* **76**, 290 (1967).
- ¹⁸B. C. Lu, S.-D. Chang, I. M. Elshayal, P. Yu, D. Gravelle, and D. P. L. Poon, in *Proceedings of the 1st International Conference on Calorimetry Thermodynamics*, Warsaw, 1969.
- ¹⁹W. Forg and P. Wirtz, *Linde Rep. Sci. Technol.* **15**, 46 (1970).
- ²⁰V. G. Skripka, I. E. Nikitina, L. A. Zhdanovich, A. G. Sirotnin, and O. A. Benyaminovich, *Gazov Promst.* **15** (12), 35 (1970).
- ²¹R. C. Miller, A. J. Kidnay, and M. J. Hiza, *AIChE J.* **19**, 145 (1973).
- ²²W. R. Parrish and M. J. Hiza, *Adv. Cryog. Eng.* **19**, 300 (1974).
- ²³R. Stryjek, P. S. Chappellear, and R. Kobayashi, *J. Chem. Eng. Data* **19**, 334 (1974).
- ²⁴A. J. Kidnay, R. C. Miller, W. R. Parrish, and M. J. Hiza, *Cryogenics* **15**, 531 (1975).
- ²⁵G. M. Wilson, *Adv. Cryog. Eng.* **20**, 164 (1975).
- ²⁶O. W. McClure, K. L. Lewis, R. C. Miller, and L. A. K. Staveley, *J. Chem. Thermodyn.* **8**, 785 (1976).
- ²⁷Yu. Blagoi, *Ukr. Fiz. Zh. (Russ. Ed.)* **4**, 577 (1959).
- ²⁸S. Fuks and A. Bellemans, *Bull. Soc. Chim. Belg.* **76**, 290 (1967).
- ²⁹Y.-P. Liu and R. C. Miller, *J. Chem. Thermodyn.* **4**, 85 (1972); R. Massengill and R. C. Miller, *J. Chem. Thermodyn.* **5**, 207 (1973).
- ³⁰J. B. Rodosevich and R. C. Miller, *AIChE J.* **19**, 729 (1973).
- ³¹M. J. Hiza, W. M. Haynes, and W. R. Parrish, *J. Chem. Thermodyn.* **9**, 873 (1977).

- ³²M. Nunes da Ponte, W. B. Streett, and L. A. K. Staveley, *J. Chem. Thermodyn.* **10**, 151 (1978).
- ³³S. P. Singh and R. C. Miller, *J. Chem. Thermodyn.* **10**, 747 (1978).
- ³⁴S. P. Singh and R. C. Miller, *J. Chem. Thermodyn.* **11**, 395 (1979).
- ³⁵F. G. Keyes and H. G. Burks, *J. Am. Chem. Soc.* **50**, 1100 (1928).
- ³⁶D. M. Mason and B. E. Eakin, *J. Chem. Eng. Data* **6**, 499 (1961).
- ³⁷A. G. Blake, R. H. Bretton, and B. F. Dodge, *AIChE Symp. Ser.* **2**, 105 (1965).
- ³⁸J. Brewer, Midwest Research Institute, Kansas City, MO, Report No. MRL-2915-C, AFOSR-67-2795, DDC No. AD 663 448, 1967.
- ³⁹D. R. Roe, Ph.D. thesis (University of London, Imperial College, London, 1972).
- ⁴⁰A. I. Semanova, E. A. Emelyanova, S. S. Tsimmerman, and D. S. Tsiklis, *Zh. Fiz. Khim.* **53** (4), 923 (1979).
- ⁴¹G. C. Straty and D. E. Diller, *J. Chem. Thermodyn.* **12**, 937 (1980).
- ⁴²W. M. Haynes and R. D. McCarty, *J. Chem. Thermodyn.* **15**, 815 (1983).
- ⁴³R. T. Jacobsen, R. B. Stewart, R. D. McCarty, and H. J. M. Hanley, *Natl. Bur. Stand. (U. S.) Tech. Note* 648 (1973).
- ⁴⁴R. D. Goodwin, *Natl. Bur. Stand. (U. S.) Tech. Note* 653 (1974).
- ⁴⁵J. A. Barker, *Aust. J. Chem.* **6**, 207 (1953).
- ⁴⁶J. M. Prausnitz, *Molecular Thermodynamics of Fluid Phase Equilibria* (Prentice-Hall, Englewood Cliffs, 1969).
- ⁴⁷H. C. Van Ness and M. M. Abbott, *Classical Thermodynamics of Non Electrolyte Solutions With Applications to Phase Equilibria* (McGraw-Hill, New York, 1982).
- ⁴⁸R. D. Gunn, T. Yamada, and D. Whitman, *AIChE J.* **20**, 906 (1974).
- ⁴⁹L. J. Christiansen and A. Fredenslund, *AIChE J.* **21**, 49 (1975).
- ⁵⁰G. C. Straty and D. E. Diller, *J. Chem. Thermodyn.* **12**, 927 (1980).
- ⁵¹R. D. McCarty, *Cryogenics* **14**, 276 (1974).
- ⁵²S. P. Singh and R. C. Miller, *Adv. Chem. Ser.* **182**, 323 (1979).
- ⁵³R. D. McCarty, *Natl. Bur. Stand. (U. S.) Tech. Note* 1030 (1980); *J. Chem. Thermodyn.* **14**, 837 (1982).
- ⁵⁴D.-Y. Peng and D. B. Robinson, *Ind. Eng. Chem. Fundam.* **15**, 59 (1976).

Appendix A. Calculational Method Used to Obtain g^E Values from $PTxy$ Data

At equilibrium the fugacities of each component in the liquid and vapor phases must be equal,

$$f_i^L = f_i^V \quad (\text{A1})$$

From the equality of component fugacities in the equilibrium vapor and liquid phases, the symmetric-convention form of the phase equilibrium relation can be written as

$$y_i \phi_i P = f_{\text{pure } i}^{(P^r)} \gamma_i^{(P^r)} x_i \exp \int_{P^r}^P \frac{\bar{V}_i dP}{RT}, \quad (\text{A2})$$

where

$$f_{\text{pure } i}^{(P^r)} = P_i^s \phi_i^s \exp \int_{P_i^s}^{P^r} \frac{V_i dP}{RT}. \quad (\text{A3})$$

The assumptions used in applying the equations are:

(1) The liquid molar and partial molar volumes are independent of pressure.

(2) The Peng-Robinson⁵⁴ equation of state can be used to calculate ϕ_i , ϕ_i^s , and \bar{V}_i .

(3) The mixing rules for the Peng-Robinson equation are:

$$a = y_1^2 a_{11} + 2y_1 y_2 a_{12} + y_2^2 a_{22}$$

$$b = y_1^2 b_{11} + 2y_1 y_2 b_{12} + y_2^2 b_{22}$$

and the combining rules are:

$$a_{12} = (a_1 a_2)^{1/2} (b_{12}^2 / b_1 b_2)^{1/2} (1 - k_{12}),$$

$$b_{12} = \left[\frac{1}{2} (b_{11}^{1/3} + b_{22}^{1/3}) \right]^3 (1 - j_{12}).$$

The values of the activity coefficient at zero pressure, $\gamma_i^{(P^r)}$, obtained from Eqs. (A2) and (A3) are then used to obtain g^E with the relation

$$g^E/RT = \sum_i x_i \ln \gamma_i^{(P^r)}. \quad (\text{A4})$$

The individual g^E values are then fit to a three-term Redlich-Kister equation to obtain the g^E value for the equimolar mixture.

Appendix B. Isotherm Generation from the Data of Bloomer and Parent (Ref. 7)

Bloomer and Parent⁷ report only dew-point and bubble-point data. Figure 8 of that reference indicates a nearly linear plot of the logarithm of bubble-point (or dew-point) pressure versus reciprocal absolute temperature. Kidnay *et al.*²⁴ fit the Bloomer and Parent bubble-point data to the equation

$$\ln P = A + \frac{B}{T} + \frac{C}{T^2} \quad (\text{B1})$$

with P in psia and T in Rankine, as reported in the original work. This work refit the data to the above equation, with the resulting coefficients and statistical parameters listed in Table B-1. For isotherms of interest Eq. (B1) was used to generate bubble-point or dew-point pressures at the composition of the liquid or vapor phase studied by Bloomer and Parent.

Table B-1
Summary of Fit of Bloomer and Parent's N_2 - CH_4 VLE Data

$\ln P(\text{psia}) = A + \frac{B}{T(\text{R})} + \frac{C}{T^2(\text{R}^2)}$						
mole % CH_4	DP or BP	A	B	C	Corre- lation coeff.	Standard error estimate
98.58	DP	12.9741	-2,456.12	83,580.05	0.99998	3.99×10^{-3}
+	BP	12.6996	-2,346.56	80,318.28	0.99990	8.41×10^{-3}
97.05	DP	13.1455	-2,545.70	97,133.90	0.99997	4.83×10^{-3}
+	BP	12.8274	-2,473.86	112,625.47	0.99989	3.00×10^{-3}
93.89	DP	13.1841	-2,540.17	96,979.61	0.99974	1.58×10^{-2}
+	BP	12.2249	-2,163.89	85,240.62	0.99917	7.43×10^{-3}
89.98	DP	12.9669	-2,326.39	56,999.76	0.99912	1.81×10^{-2}
+	BP	11.7582	-1,931.50	69,021.73	0.99977	9.23×10^{-3}
71.2	DP	13.5045	-2,407.01	60,609.50	0.99981	2.73×10^{-2}
+	BP	10.2995	-1,137.83	-3,277.19	0.99991	1.72×10^{-2}
49.12	DP	14.2501	-2,495.63	62,456.86	0.99979	3.036×10^{-2}
+	BP	9.2875	-566.25	-61,586.85	0.99942	3.51×10^{-2}
30.3	DP	15.365	-2,733.83	84,467.50	0.99978	2.99×10^{-2}
+	BP	9.4475	-542.93	-64,636.64	0.99948	3.06×10^{-2}
15.77	DP	13.8025	-1,884.64	2,890.84	0.99977	3.01×10^{-2}
+	BP	10.0844	-706.83	-51,668.30	0.99977	1.70×10^{-2}
4.85	DP	13.2095	-1,717.76	20,297.58	0.99997	7.86×10^{-3}
+	BP	11.6026	-1,243.02	-913.998	0.99997	6.00×10^{-3}
0	both	13.4556	-1,930.52	64,528.31	0.999994	3.22×10^{-3}
100	both	12.0513	-1,940.25	11,527.21	0.999978	9.73×10^{-3}